Revealing Monoamine Oxidase B Catalytic Mechanisms by Means of the Quantum Chemical Cluster Approach

Gerald Zapata-Torres,*,[†] Angélica Fierro,[‡] German Barriga-González,[§] J. Cristian Salgado,[‖] and Cristian Celis-Barros[§]

[†]Molecular Graphics Suite, Department of Inorganic and Analytical Chemistry, Faculty of Chemical and Pharmaceutical Sciences, University of Chile, Santiago, Chile

[‡]Facultad de Química, Departamento de Química Orgánica, Pontificia Universidad Católica de Chile, Santiago, Chile

[§]Universidad Andres Bello, Facultad de Ciencias Exactas, Departamento de Ciencias Quimicas, Avenida República 275, 8370146 Santiago, Chile

[‖]Laboratory of Process Modeling and Distributed Computing, Department of Chemical Engineering and Biotechnology, University of Chile, Beauchef 850, Santiago, Chile

S *Supporting Information*

ABSTRACT: Two of the possible catalytic mechanisms for neurotransmitter oxidative deamination by monoamine oxidase B (MAO B), namely, polar nucleophilic and hydride transfer, were addressed in order to comprehend the nature of their rate-determining step. The Quantum Chemical Cluster Approach was used to obtain transition states of MAO B complexed with phenylethylamine (PEA), benzylamine (BA), and *p*-nitrobenzylamine (NBA). The choice of these amines relies on their importance to address MAO B catalytic mechanisms so as to help us to answer questions such as why BA is a better substrate than NBA or how *para*-substitution affects substrate's reactivity. Transition states were later validated by comparison with the experimental free energy barriers. From a theoretical point of view, and according to the our reported transition states, their calculated barriers and structural and orbital differences obtained by us among these compounds, we propose that good substrates such as BA and PEA might follow the hydride transfer pathway while poor substrates such as NBA prefer the polar nucleophilic mechanism, which might suggest that MAO B can act by both mechanisms. The low free energy barriers for BA and PEA reflect the preference that MAO B has for hydride transfer over the polar nucleophilic mechanism when catalyzing the oxidative deamination of neurotransmitters.
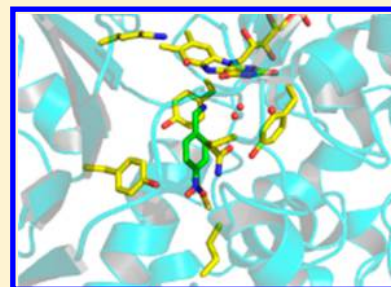
INTRODUCTION

Monoamine oxidases (MAOs) are a family of flavin-containing enzymes that catalyze the oxidative deamination of neurotransmitters, essentially serotonin, dopamine, and noradrenaline.[1] In humans, two isoforms exist, MAO A and MAO B, and their available crystal structures exhibit similar Cα chain folds as expected according to their high sequence identity (ca. 70%).[2] Also, their active sites are almost indentical, except for a few aminio acids such as Tyr326, Cys172 and Ile199 in MAO B (Ile 335, Asn181 and Phe208 in MAO A). As a result, it has been argued that their FAD sites are essentially identical, leading to the common statement that both enzymes catalyze amine oxidation by identical mechanisms.

Several mechanisms involved in MAO catalysis have been proposed, namely, polar nucleophilic[3] (PN) (Scheme 1a), single electron transfer[4,5] (SET) (Scheme 1b), hydride transfer[6] (HT) (Scheme 1c), and two-step hydride transfer[7] (Scheme 1d) mechanisms. This last pathway has been described as energetically more feasible than the others, and it agrees well with all the available experimental data including the positive and negative Taft correlation experiments carried out by Edmondson et al.[8] In the past few years, the SET mechanism

was discarded, although in a recent article it has been suggested that it should be reconsidered.[9] In 2011, Erdem et al. published a computational study presenting negative evidence for the SET mechanism.[10] The PN and HT mechanisms have been widely discussed in order to shed light on the nature of the experimental rate-determining step. For instance, Orru et al.[8] addressed the dilemma regarding the same or different mechanisms for both MAO isoforms. Abad et al.[11] used computational chemistry to favor the PN mechanism. Vianello et al.[7] were the first to show computationally the prevailing feasibility of the HT over all other mechanisms, suggesting that this two-step hydride transfer mechanism might operate in MAO B. However, as stated by the authors considering the structural resemblances of both isoforms, i.e. similarities in their active-site region, identical FAD cofactors, equally good metabolization of a large variety of substrates, "the possibility that the two enzymes function through different mechanisms is very unlikely" leaving room to think that the two-step hydride mechanism might operate both in MAO A and MAO B. This

Scheme 1. (a) Polar Nucleophilic Mechanism Involves Proton Transfer and Formation of N_{am}–C4a Adduct. (b) Single Electron Transfer Mechanism Involves Free Radical Species. (c) Hydride Transfer Mechanism Involves Direct Transfer of Hydride from Substrate Cα to Flavin. (d) Two-Step Hydride Transfer Implies Formation of Intermediate Adduct between Cα and N5.
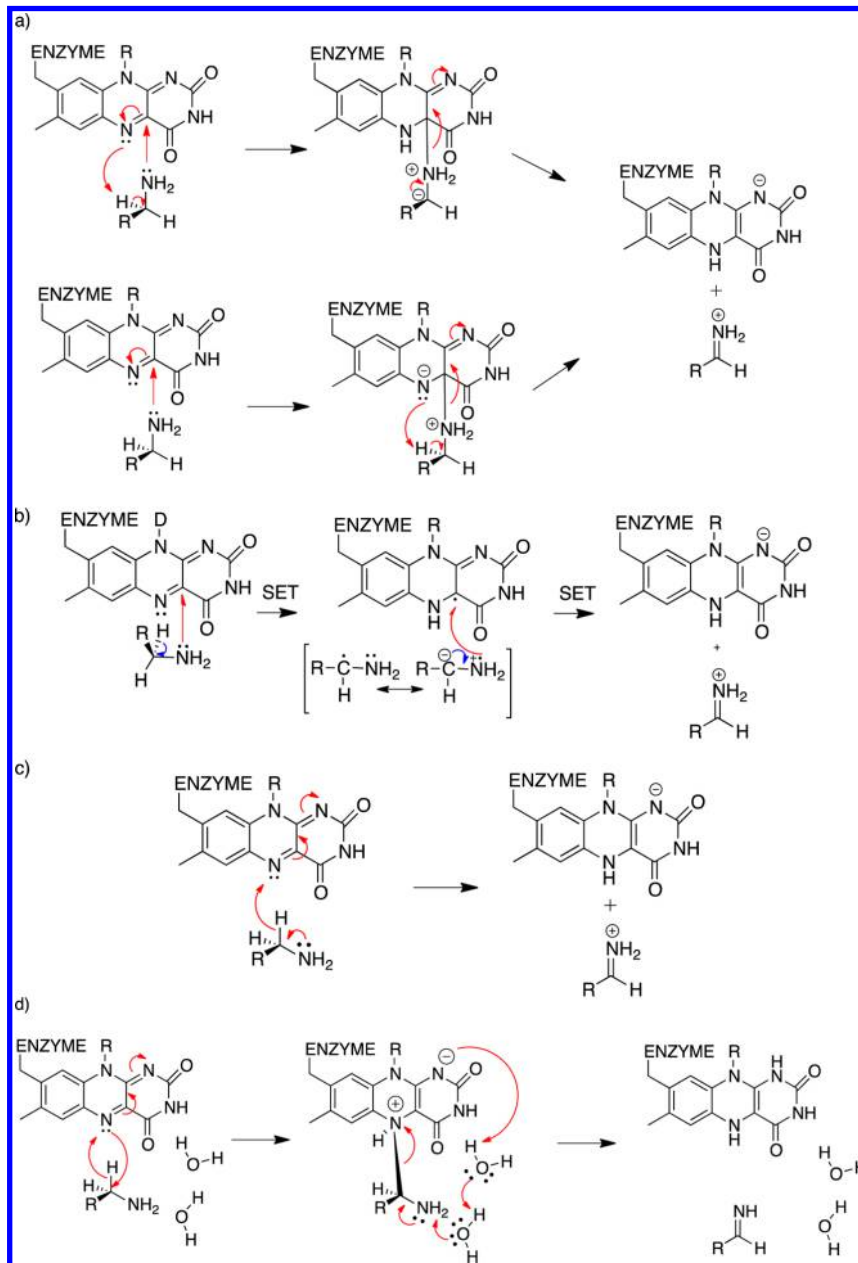
study was later extended by Repič et al.,[13] reaching the same conclusions. Finally, Akyüz et al.,[12] using computational modeling to find transition states in MAO B, also favored the HT pathway.[12] In the latter work, formation of the Cα–flavin N5 adduct in MAO studied using the M06-2X functional revealed that this only occurs in MAO B, suggesting slightly different hydride transfer mechanisms operating in MAO A and MAO B.[12]

Due to its pivotal role in neurotransmitter degradation, the determination of MAO catalytic mechanisms is of paramount importance, since it is well known that variations in MAO activity levels might trigger important psychiatric and/or neurological disorders.[2] Generally, MAO A is related to depression because of its association with the control of serotonin levels. On the other hand, MAO B has been

associated with Alzheimer's and Parkinson's diseases because this enzyme modulates dopamine levels in the CNS.[2]

Structural results of several FAD-dependent amine-oxidizing enzymes including human MAOs show that two aromatic residues in the binding site are oriented approximately perpendicular to the flavin ring forming a "cage" opening toward the entrance, suggesting their functional involvement in catalysis. Consequently, the functional role of two tyrosines (in the case of human MAO B, Tyr398 and Tyr435, Tyr407 and Tyr444 in MAO A) defining the aromatic cage has been investigated at the Hartree–Fock/MM level.[14] Also, it has been discussed that active site aromatic residues have a role in cation-π interactions.[15] These interactions have been discussed in the example of the bound protonated dopamine in MAO;[7] however, this does not seem to occur with serotonin and

MAO inhibitors according to our previous results[16] and other catalytic proposals such as those described by Repič et al.[17] and references cited therein. In the case of human MAO B, the tyrosine side chains project into the substrate binding cavity on the *Re* face of the covalently bound flavin ring.[18] This aromatic cage arrangement might influence the catalysis by eliciting inductive effects on the substrate's amine nitrogen atom favoring the abstraction of the neighboring hydrogen. Furthermore, a conserved lysine residue (Lys296 in MAO B, Lys305 in MAO A) is located in a solvent-inaccessible hydrophobic area of the active site, establishing a well conserved Lys-water-N5 motif that is also found in other oxidases.[19] However, this conserved motif would be expected to fluctuate, with water molecules easily leaving and entering the active site, since the free energy cost linked to water displacement from and to the active site is small relative to the chemical step. In this situation, the lysine amino group should be subjected to strong electrostatic effects that might alter its acid/base equilibrium. In fact, similar results have been obtained with other oxidases, where the corresponding conserved lysine residues remain unprotonated upon substrate binding, judging from both experimental and theoretical work.[20]

Repič et al.[13] have shown that the pK_a of Lys296 with dopamine docked into the active site of MAO B is 10.8. They have indicated that this residue is mainly present in its charged form at the physiological pH, positing that this preferred ionization state is not the catalytically active one indicating that the reaction barrier for the reaction does not really depend on the Lys296 protonation state. Thus, the protonation state of this residue would not affect the reductive half-reaction of MAO B. As a matter of fact, Borštnar et al.[21] demonstrated that the pK_a value of dopamine in the MAO B active site is practically identical to the figure in aqueous solution (8.8 and 8.9, respectively), indicating that the cost of deprotonating dopamine is low and its deprotonation is easily achieved in the protein's internal environment.[21]

On the other hand, for MAO substrates, although the cationic species is dominant under physiological conditions, an active site which is not at all hydrophobic favors the unprotonated state in agreement with our previous results, indicating that a neutral substrate is needed for the reaction to take place.[16]

During the catalytic reductive half-reaction, the Cα–Hα bond of substrates is oxidatively cleaved to form a protonated imine intermediate. Then, the reduced cofactor is reoxidized to its functional form by molecular oxygen, followed by the release of hydrogen peroxide during the oxidative half-reaction. The protonated imine intermediate is finally hydrolyzed non-enzymatically to release ammonium ion and the corresponding aldehyde. Nonetheless, for most of the flavin-dependent amine oxidases, the chemical mechanism of the reductive half-reaction involving the irreversible Cα–Hα bond cleavage remains elusive. Large experimental kinetic isotope effects have been observed for some benzylamine substrates showing unequivocally that the Cα–Hα (pro-*R*) bond cleavage is the rate-limiting step under experimental conditions such as steady state and stopped flow assays with MAO A.[22] This rate-limiting step has also been found theoretically and experimentally in MAO B.[7,23] These observations agree well with experimental evidence indicating that no intermediates between the oxidized and reduced flavin are detected spectroscopically, providing indirect support for the direct HT mechanism as the preferred one in

MAO B. Extensions of the study of Vianello et al.[7] have included full dimensionality of the enzyme by means of empirical valence bond simulations including thermal corrections.[13,24]

Polar Nucleophilic Mechanism. The first computational study on the mechanism of MAO catalysis addressed the proposed polar nucleophilic mechanism by means of quantum chemical calculations employing the semi-empirical PM3 method.[25] Mechanistic evidence supporting a PN mechanism for MAO A catalysis has also been discussed elsewhere.[8] In this mechanism, the –NH$_2$ moiety of the bound substrate in its deprotonated form attacks the C4a position of the isoalloxazine ring to form a flavin C4a adduct. The basic N5 of this adduct eventually abstracts the Cα–Hα from the substrate (Scheme 1a).[8]

Abad et al.,[11] using benzylamine as the MAO B substrate, described an asynchronous PN mechanism (lower pathway in Scheme 1a). This mechanism describes the amine moiety's lone pair (N$_{am}$) interaction with C4a of the isoalloxazine ring at a rather short distance (ca. 2.52 Å). The authors thus evidenced an optimal distance between N$_{am}$ and C4a, claiming that this interaction is an attractive one; however, they indicated that it is too long for a covalent bond although short enough for a normal nonbonded distance. The study also suggested that the concerted, but asynchronous, transfer of two electrons and a proton in the rate-limiting step is in agreement with the PN mechanism. It should be noted that a similar asynchronous concerted polar nucleophilic mechanism was initially suggested by Erdem et al.[25]

Hydride Transfer Mechanism. Other studies with flavin-dependent amine oxidizing enzymes have proposed a Cα–Hα bond cleavage by means of a hydride ion mechanism (Scheme 1c).[6] According to this proposal, electron donation from the amine nitrogen to the Cα–N$_{am}$ bond of the substrate facilitates departure of a hydride ion from Cα to the flavin N5 in a single step.[6] On the other hand, using quantum chemical calculations, a novel two-step hydride mechanism for the oxidative MAO-catalyzed deamination of amines has been proposed (Scheme 1d)[7] In this proposal, during the rate-limiting step, the flavin abstracts a hydride anion (through its N5 atom) from the substrate's α-carbon. Then, a strong covalent adduct is formed between the Cα and N5. In a later stage, a facilitated deprotonation of the adduct by two active-site water molecules would produce a fully reduced flavin, FADH$_2$, and a neutral imine.[7] Experimentally, this two-step HT was shown to be energetically more feasible compared to other mechanistic pathways.[8] Recent ^{15}N kinetic isotope effect measurements of human MAO B oxidation of benzylamine show that Cα–Hα bond cleavage and N$_{am}$-rehybridization are not concerted, which argues against a direct hydride mechanism for MAO B.[23] However, it has been suggested that the two-step hydride transfer mechanism might only operate in MAO B but not in MAO A.[12]

Despite the structural resemblance of both active sites, the electrostatic environment in MAO A and MAO B should not be identical, allowing for different degrees of charge transfer in the reactant complexes upon formation. In this context, Abad et al.[11] described that MAO A performs the oxidative deamination of amines by a PN mechanism in contrast to the HT used by MAO B. The same authors[24] have recently claimed that the reaction rate is influenced by the N$_{am}$–C4a interaction, and substituent effects on substrates only play a minor role, indicating that active site environmental effects bring the

pathway closer to an asynchronous PN mechanism in MAO B. However, in a computational study for the oxidation of benzylamine by flavin,[26] it was concluded that both mechanisms might be operating in MAO due to very similar energy barriers for the PN and HT mechanisms.

All the mechanisms depicted in Scheme 1 show a protonated imine product, which agrees with the experimental evidence showing that the imine product is in its protonated state.[27,28]

Despite of the ongoing discussion regarding alternative mechanisms in MAO, it would seem unlikely that such closely related enzymes would employ different mechanistic strategies to accomplish very similar amine oxidations.[21] In fact, to carry out such a task, two different active site electrostatic preorganizations would have to occur in order to stabilize transition states involving a carbanion in MAO A or a carbocation in MAO B. In this context, the Quantum Chemical Cluster Approach can be used as a robust tool with the aim of rationalizing the accumulated experimental evidence for these enzymes.[29,30] The Quantum Chemical Cluster Approach allows the confirmation of transition states that are difficult to find and/or be characterized through experiment. By means of potential energy profiles, the experimental rate-limiting steps can be studied and their associated energy barriers can be obtained. Also, several reaction pathways can be compared with experimental kinetic results to shed further light on the possible mechanism.

Although theoretical calculations regarding MAO mechanisms abound, several disadvantages can be noted due to the solvent not being included, such as long-range polarization effects and steric constraints imposed by the enzyme on the substrates. However, these disadvantages are overruled by using the Quantum Chemical Cluster Approach.[31] Also, most earlier calculations do not reproduce experimental $k_{cat/red}$ values, failing by ca. 8−10 kcal/mol. Therefore, the main focus of this work is a thorough understanding of the chemical steps of amine degradation and the basis of the catalytic power of MAO B, which would be of great importance for other studies on flavoenzymes. As has been pointed out,[26] a detailed knowledge of MAO catalytic activity is important for the effective design of novel MAO inhibitors as transition state analogues so as to determine how these enzymes work.

■ RESULTS AND DISCUSSION

Free Energies of Activation and Kinetic Values. In this article we report the localization and characterization of transition states by comparison of calculated energy barriers derived from potential energy profiles ($\Delta G_{cat}^{\neq}$) and those obtained through available experimental kinetic parameters (k_{red}) for three selected arylalkylamine analogue MAO B substrates, namely benzylamine (BA), phenylethylamine (PEA) and *p*-nitrobenzylamine (NBA) (Figure 1).

These results were used to analyze and investigate the likelihood of a particular reaction pathway to occur, i.e. to rationalize the PN versus the HT mechanism in MAO B. To accomplish this, experimental free energies of activation ($\Delta G_{exp}^{\neq}$) were obtained by means of the Eyring equation as shown in Table 1 (see Methodology section). Then, we used an alternative methodology to the QM/MM approach, which considers QM-only calculations of a suitable and well-chosen active-site model as described by Siegbahn et al.[31]

It should be noted that a variation of $\Delta G_{exp}^{\neq}$ of 1.4 kcal/mol in Table 1 leads to a decrease in catalytic effectiveness in 1 order of magnitude, as described elsewhere.[32]
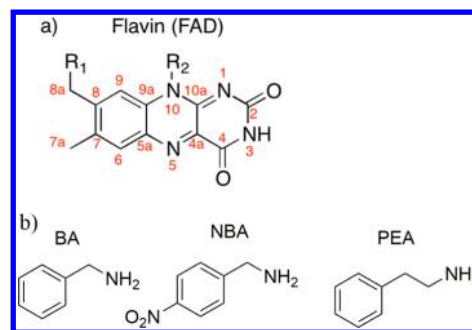

Figure 1. a) Atom numbering of the flavin moiety of FAD and b) structures of the substrates used in this study.

Table 1. Free Energy of Activation $\Delta G_{exp}^{\neq}$, $\Delta G_{cat}^{\neq}$ (Table S2, Supporting Information), and $\Delta G_{w}^{\neq}$ (in solution) for Arylalkylamine Analogues as MAO B Substrates Using the Quantum Chemical Cluster Approach

substrate	k_{red} (min^{-1})	$\Delta G_{exp}^{\neq}$	$\Delta G_{cat}^{\neq}$	$\Delta G_{w}^{\neq}$
benzylamine	760 ± 2^a	16.0	19.4	31.7
phenethylamine	34300^b	13.7	17.1	31.1
p-nitrobenzylamine	3.8 ± 0.2^a	19.1	18.5	30.5

^{a}Taken from ref 33. ^{b}Taken from ref 34.

The data in Table 1 show the stopped-flow kinetic parameters of MAO B reported for the oxidation of BA, PEA, and NBA.[33,34] As Edmondson et al.[35] have discussed, NBA is found to be a very slow substrate for MAO B, indicating that it might function as a competitive inhibitor. BA and PEA are found to be good MAO B substrates. Thus, the choice of these molecules relies on their importance to address the possible catalytic mechanisms in this enzyme. Also, this choice could help us to answer questions such as why BA is a better substrate than NBA or how *para*-substitution in the aromatic ring affects the substrate's reactivity or even if other substrates might follow the same oxidative mechanisms.

It is worth mentioning that higher calculated energy barriers (over 25 kcal/mol) often imply that either the mechanism is wrong or probably the model is missing something or contains some artifacts.[36] According to this, our calculated free energy of activation for NBA is in excellent agreement with its experimental value. On the other hand, in the case of BA and PEA, these energies are overestimated by ca. 3 kcal/mol even though these results show the same trend as the experimental values, i.e., the barrier for BA is 2.3 kcal/mol higher than for PEA. A possible explanation for this observation is that calculations carried out using NBA were based on the MAO B−NBA crystal structure (PDB code 2C70),[35] implying that the amino acid residues are arranged according to the interactions with this substrate.

Catalytic Power of MAO B. An efficient way to evaluate the origin of enzyme catalysis is to use the catalytic power parameter described elsewhere.[37,38] Usually, this is carried out using experimental kinetic values that represent the catalytic power k_{cat}/k_{uncat} (k_{red}/k_{uncat} ratio in our case) for enzymes, which lie between 10^6−10^{17}, meaning 9.5−26 kcal/mol in terms of $\Delta\Delta G^{\neq}$ values (eq 1, see Methodology section).

Thus, the difference between $\Delta G_{w}^{\neq}$ and $\Delta G_{cat}^{\neq}$ (Table 1) results in the catalytic power, $\Delta\Delta G^{\neq}$. According to our calculations, MAO B enhances the reaction rate up to 10^{10} times with regard to the uncatalyzed reaction in water. Despite the lack of experimental data regarding the uncatalyzed reaction
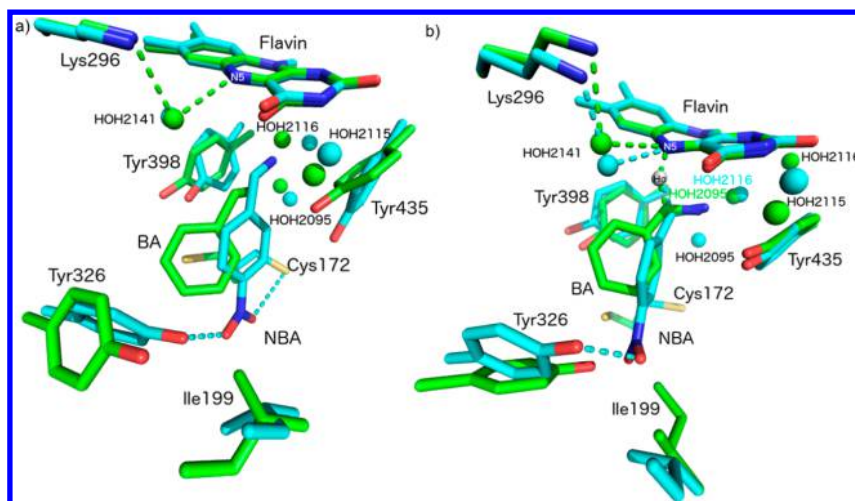
Figure 2. Molecular overlay of (a) reactant complexes (RC) and (b) transition states (TS) of NBA (cyan) and BA (green). For the sake of clarity, Gln206 was deleted from the picture and the oxygens of water molecules (depicted as spheres) were colored the same as carbon atoms and numbered according to crystal structure 2C70.

Figure 3. Molecular overlay of (a) reactant complexes (RC) and (b) transition states (TS) of PEA (magenta) and BA (green). For the sake of clarity Gln206 was deleted from the picture and the oxygens of water molecules (depicted as spheres) were colored the same as carbon atoms and numbered according to crystal structure 2C70.
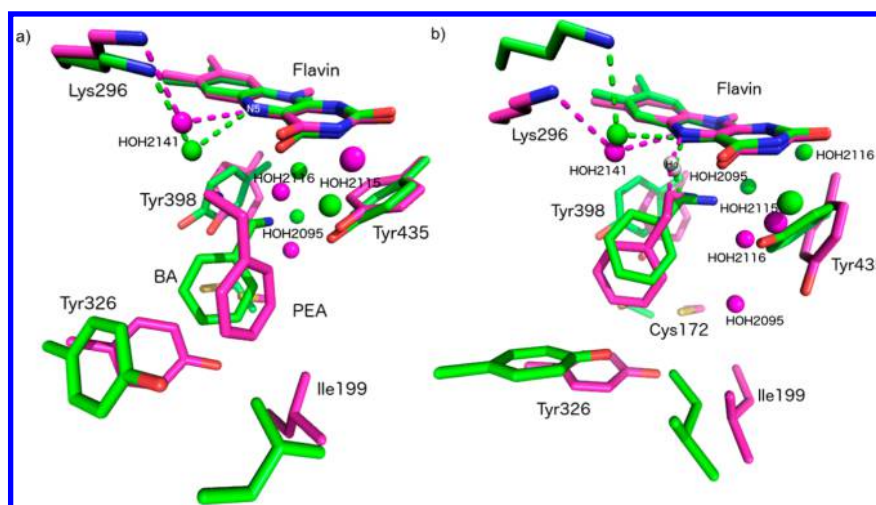
(from amine to imine), our results are in agreement with the reported experimental range of values for natural enzymes.[37] Thus, comparisons of nonenzymatic with catalyzed reactions should give us new hints regarding the mechanistic pathway followed by the MAO B catalyzed reaction.

Transition State Stabilization (TSS). According to Warshel et al.,[38] the catalytic effect of enzymes resides essentially in the electrostatic stabilization of the transition state rather than several other proposed features (strain, entropy, desolvation, tunneling, covalent effects, dynamics, among others). All these proposals attempt to explain the catalytic effect. Therefore, in this context, our discussions are focused on the comparison between the TS and RC states.

p-Nitrobenzylamine. Edmondson et al.[35] suggested that dipolar properties of residues Tyr398 and Tyr435 (Figure 2) play an important role in substrate specificity for MAO B catalysis. Also, experimental data on p-NO$_2$ substrate analogues indicated that repulsive interactions might alter the orientation of these substrates in the active site cavity with regard to these two tyrosine residues. If so, the latter statement could explain

the poor behavior displayed by NBA as a MAO B substrate. Moreover, it is worth noting that it binds tightly to the active site as shown by crystal structure reports.[35]

Due to the fact that the RC state for NBA was obtained from an optimization of a well-chosen region of the crystal structure of MAO B (see Methodology section), some differences could be seen regarding the crystal state. The main discrepancy can be noticed in the −NO$_2$ group, that shows a hydrogen bond with Tyr326 (Figure 2a) that is not present in the crystal structure (where it interacts with Cys172 at 3.07 Å). We believe that in a dynamic system both interactions might be present. Whether one or both of these interactions occur, the NBA will remain anchored at the entrance cavity. Although NBA is a simple derivative of the good substrate BA, the interactions of the −NO$_2$ group may be responsible for the decreased reactivity of NBA regarding BA. The anchoring of NBA may decrease its likelihood of adopting an appropriate conformation to interact with the flavin moiety (near attack conformation[38]).
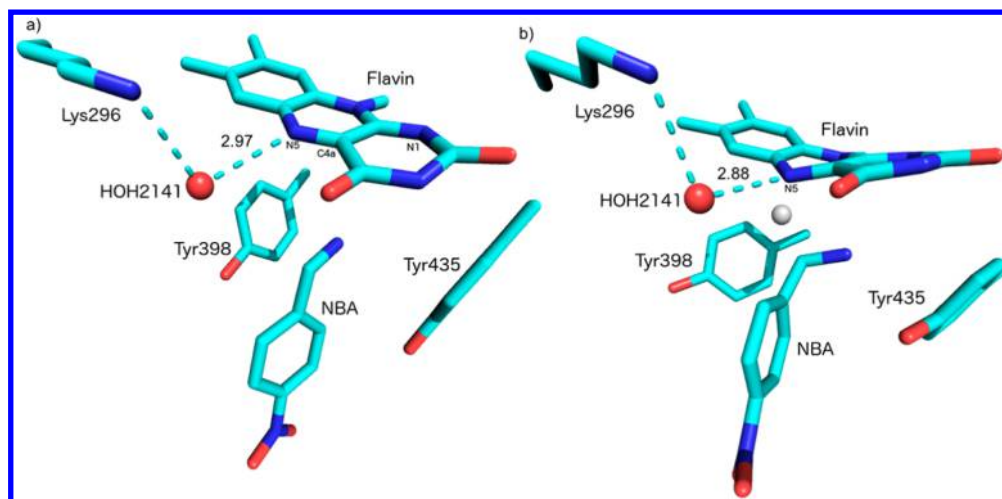
Figure 4. (a) Reactant complex and (b) transition state forNBA. The image shows the Lys296−HOH2141−N5 motif and how the water molecule approaches N5 on going from the RC to the TS. For the sake of clarity, Gln206, Tyr326, Ile199, and Cys172 are not shown in the figure. Only HOH2141 was left and named according to crystal structure 2C70.

The interactions occurring in the TS (Table S1, Supporting Information) show that NBA is similarly stabilized with regard to BA and PEA.

Benzylamine. Kinetic and thermochemical differences between BA and its derivative NBA could be explained by the absence of the Tyr326−Cys172 anchoring. Instead of this interaction, π−π and polar−π interactions are observed in the RC of BA (Figures 2a and 3a). The first interaction forms an angle of 36.25° (measured from the normal vector of Tyr326 to the centroid of the BA) at a distance of 5.38 Å (measured between aromatic ring centroids), which is in agreement with described π−π interactions in proteins.[39] A second interaction is observed between the thiol group of Cys172 and the benzyl ring of BA at 2.3 Å, forming an angle of 98.8° (optimal for this kind of interactions in proteins).[39] These interactions allow BA to be pushed into the reactive region assisted by the Tyr326 and Ile199 residues located at the entrance gate in MAO B,[40] thus avoiding its anchoring at the entrance cavity. On the other hand, the analysis of the TS structure (Figures 2b and 3b) clearly shows that the number of interactions in the active site increase regarding the ground state structure (Table S1, Supporting Information), i.e., three new H-bonds are formed in the TS and six H-bonds become shorter as compared to the ground state, confirming the stronger interactions occurring in the BA MAO B TS complex. The higher activity displayed by BA could then be explained as due to these π interactions acting as a driving force. In this way, BA is more likely to reach the TS and achieve the tighter interactions observed in the TS structure (Table S1, Supporting Information).

Phenylethylamine. According to the kinetic data (Table 1), simply increasing the length of the side chain by an extra methylene group, as is the case for PEA, increases its reactivity regarding BA. Also, this methylene group allows PEA to adopt a more favorable conformation in the active site in the RC (similar to the TS), i.e., allowing PEA to orient its Hα toward the N5 of the flavin (Figure 3). Additionally, similar π interactions are observed as in the case of BA, and therefore, they could assist the approach of Cα toward N5. Moreover, the interactions found for PEA in the RC and TS are almost the same (Table S1, Supporting Information). These similarities between both the RC and TS in Figure 3 might explain the

increased reactivity and the lower energy barrier calculated for this substrate.

Reactive Region and Lys296−HOH−N5 Motif. In the search for transition state structures, the water molecules considered in the linear transit (see Methodology section) form a hydrogen bond network. One of these water molecules connects the NH$_2$ group of Lys296 and the N5 of the isoalloxazine ring of FAD (Figure 4a). Interestingly, this is a conserved motif found in other oxidases but without any discussed role in MAO.[41,42] This Lys−HOH−N5 motif is conserved in all the calculated reactant and transition state complexes. Distances between this water and N5 of the isoalloxazine ring of FAD are ca. 3.0 Å in all our RC. Although in the obtained TS complexes for BA and PEA this distance is conserved at 3.0 Å, for NBA the water molecule moves toward N5 and the distance decreases to 2.88 Å as shown in Figure 4b.

Thus, based on orbitalary results (*vide infra*), it is possible to think of an enrichment of the charge of N5 arising from a local electrostatic contribution by another region of the flavin moiety.

Reactive Region. In the obtained reactant complexes, the amino moieties of BA and PEA remain far from the flavin's C4a at 3.3 and 4.1 Å, respectively. However, this distance is somewhat different in the reactant complex of NBA, depicted in Figure 2a, compared to the good substrates. In this case, the −NH$_2$ moiety binds in the binding cavity where it remains ca. 3.15 Å away from C4a of the isoalloxazine ring. Also, in this conformation of NBA, the Cα atom of the substrate remains 3.74 Å away from N5, closer than the distances attained by BA and PEA, which are 4.57 and 4.41 Å, respectively. This position is better explained by additional hydrogen bond interactions of the p-NO$_2$ substituent with the hydroxyl group of Tyr326 at 2.88 Å (Table S1, Supporting Information).

On the other hand, it is worth mentioning that in the TS complex, the −NH$_2$ group of NBA comes closer to the C4a of the isoalloxazine ring (2.53 Å). This distance in the BA and PEA complexes is 2.9 Å, which does not agree with the PN mechanism (2.52 Å) described for MAO B.[10] Thus, only NBA displays this interaction at too large a distance for a covalent bond but close enough to be considered as an attractive interaction.[11]
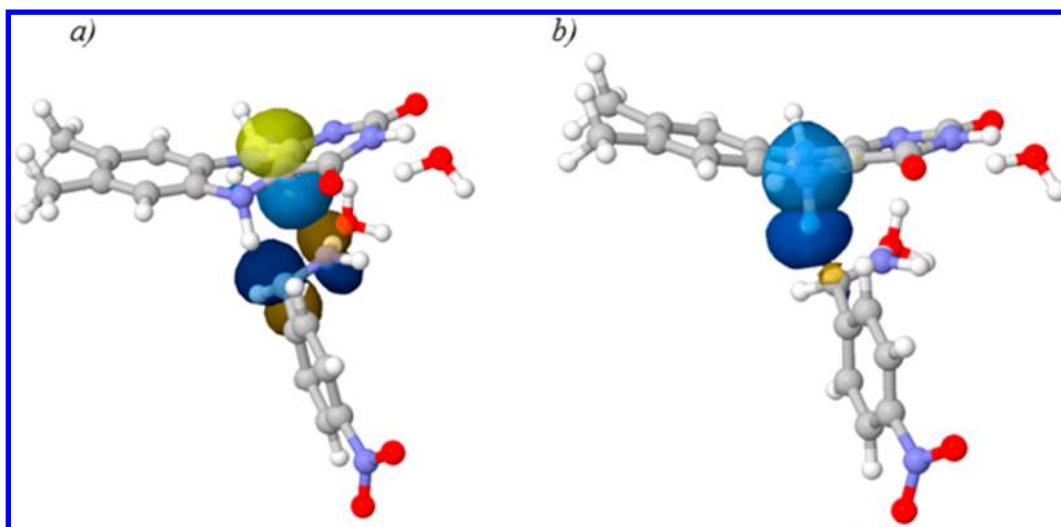
Figure 5. Graphical description of natural bond orbitals in the transition state of NBA−flavin: (a) N_{am}−Cα and C4a and (b) N5 and the transferred proton.

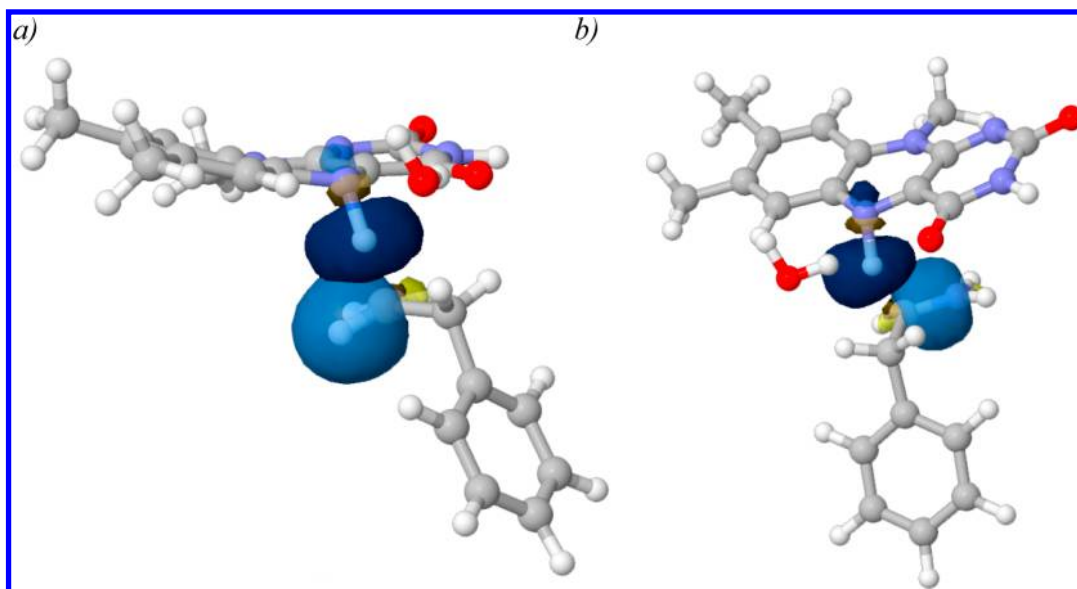**Figure 6.** Graphical description of natural bond orbitals that stabilize the Hα in the PEA TS structure: (a) Hα stabilization through the C−H of PEA and (b) C−N bond stabilizing Hα of PEA.

Also, it is possible to observe that the interaction occurring in the Lys296−HOH−N5 motif is strengthened in the NBA transition state (Table S1, Supporting Information). We believe that the conserved water molecule may partially compensate[19] for the increased basicity of the flavin N5 as described for the PN mechanism in MAO (Scheme 1b). Thus, the lack of the N_{am}−C4a interaction in BA and PEA and the elongated HOH2141−N5 interaction lead to a more electrophilic N5, favoring hydride abstraction. Even though the N_{am}−C4a interaction is also described for NBA, the hybridization of C4a remains constant ($sp^{2.13}$, $sp^{2.09}$, and $sp^{1.91}$ in RC, TS, and PC, respectively).

NBO Analysis. NBO analyses were carried out over the corresponding Fock matrices according to second-order perturbation theory for NBA and PEA complexed with MAO B. Results for the TS structure with NBA show that the flavin moiety of FAD exhibits five intramolecular orbitals (related with the mechanism under study). Also, there are two water

molecules that may be involved and associated with the mechanism and stability of the system, which interact with NBA and the flavin ring. Finally, the establishment of two NBA−flavin orbital interactions can be seen, which seems to be important in determining the stability and the reactivity of the system.

Figure S1a of the Supporting Information shows the interaction of the orbitals of the C4a and the C10a−N1 bond orbital, which could imply a possible electron delocalization from C4a to N1. Further, C4a exhibits a bonding orbital formation between N5 and Hα (Figure S1b, Supporting Information). On the other hand, the N5 lone pair seems to stabilize the C4a−C10a bond with an electron population of 1.84 e (Figure S1c, Supporting Information), as well as N10 stabilizes the C10a−-N1 bond (Figure S1d, Supporting Information). Finally, the hydrogen transferred from NBA seems to be stabilized by the N5 lone pair. The two crystallographic waters that are involved in the electron

movement in the complex might act as electron acceptors for both the flavin moiety (Figure S2, Supporting Information) and NBA (Figure S3, Supporting Information).

Figure 5a denotes an established interaction between the $N_{am}-C\alpha$ bond orbital of NBA and C4a orbital of flavin, while Figure 5b shows the overlapping of N5−Hα orbitals.

Altogether these results (despite of more evidence is needed) allow us to believe that the direction of electron motion is toward N1 assisted by a water molecule (HOH2216) as an electron acceptor with N5 acting as a base, which abstracts a proton from NBA (noticed by Vianello et al.[7]). Also, C4a of the flavin and the other water molecule (HOH2115) could stabilize the amine moiety of NBA. These results are in agreement with the PN mechanism for this substrate.

The study of the PEA TS complex shows similar orbital behavior for flavin to that seen for NBA (Figure S2, Supporting Information). However, there are several different orbitals regarding the NBA case supporting the HT over the PN mechanism. First, the pro-R Hα seems to be stabilized by the $C\alpha-H\alpha$ (pro-S) bond together with the electronic contribution from the $N_{am}-C\alpha$ bond (Figure 6). The latter could be in agreement with the electrodonation from N_{am} toward the $C\alpha-H\alpha$ bond described elsewhere for the hydride mechanism.[7] The electron populations of both the $C\alpha-H\alpha$ (pro-S) and $N_{am}-C\alpha$ bonds are high, and therefore, they are able to transfer charge toward the pro-R Hα, allowing it to be characterized as a hydride ion. Additionally, the water molecule of the Lys296−HOH2141−N5 motif is involved in the stabilization of the hydride, which is not seen in the other case (Figure 7).
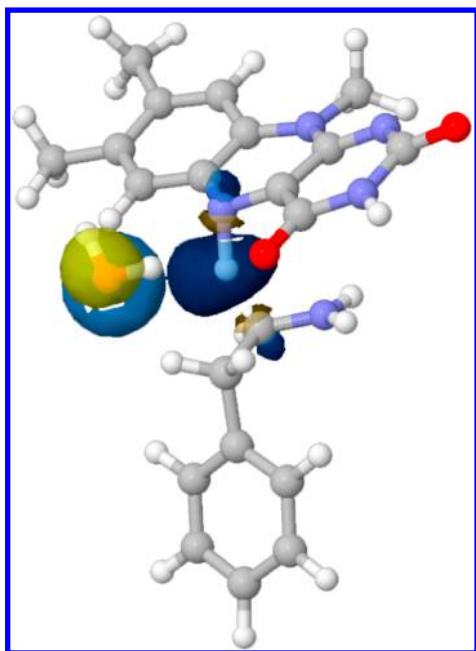

Figure 7. Graphical description of Lys−HOH2141−N(5) motif NBO orbitals that stabilize the Hα in the PEA TS structure. Hα is stabilized by an electron pair of the oxygen atom.

Importance of Crystallographic Water molecules. All crystallographic water molecules considered in our study displayed a H-bond network, making our study comparable with the available experimental data. In fact, ca. 75% of the H-bonds formed in the active site involved water molecules (Table S1, Supporting Information). As has been pointed out,

the free energy cost linked to water displacement from/to the active site is small relative to the ΔG of the reduction chemical step in accordance with the smaller penalty imposed by the enzyme active site. Moreover, the binding affinity of substrates/inhibitors may diminish if the free energy increases due to the removal of bound water molecules is not compensated by additional interactions upon their binding.[43] These water molecules are essential to represent the electrostatic behavior of the active site,[24] helping us to answer some of our mechanistic questions. Our Quantum Chemical Cluster Approach calculations support the idea that water molecules change the electrostatic environment of the active site allowing MAO B to catalyze the studied substrates by two different mechanisms. Furthermore, this importance is highlighted by the Lys296−HOH−N5 motif, which stabilizes both hydride and proton transfer. Its presence seems to favor the viability of the mechanism.[42]

Though the role of the water molecules suggests a certain degree of "mechanistic flexibility" as discussed above, the energetic and kinetic differences obtained from our calculations for good substrates as BA and PEA lead us to think that MAO B prefers the HT over the PN mechanism, while the latter might be preferred in the case of NBA.

■ CONCLUSIONS

The Quantum Chemical Cluster Approach was used as a tool aiming to rationalize gathered experimental evidence for monoamine oxidase B. Using this methodology, transition state Gibbs free energies for benzylamine, phenethylamine, and p-nitrobenzylamine complexes were obtained and compared with experimental kinetic values. The lack of crystal structures for MAO B complexed with BA and PEA may be the responsible for the small observed differences encountered in the theoretical energy barriers for BA and PEA regarding their experimental Gibbs free energies. Nevertheless, the obtained transition state structures were localized and validated, thus leading to new insights regarding the most likely mechanisms underlying the MAO B substrate interactions.

The NH_2 moiety of both BA and PEA interacted with the C4a atom of the isoalloxazine ring at a distance of 2.9 Å in the transition state complexes. In the case of NBA, its NH_2 group interacted with C4a of the isoalloxazine ring at 2.53 Å. This shorter distance argues in favor of adduct formation by the PN mechanism. In all cases the Lys296−water−N5 motif is conserved in the transition state complexes, where for BA and PEA the conserved water molecule remains at the same distance as in the reactant complexes. In contrast, in the case of NBA, the water molecule comes closer to N5 in the transition state complex. In any case, according to our NBO results, this interaction may be attributed to bond orbital formation between N_{am} and C4a only for NBA.

At a first glance, an important difference is that NBA exhibits an orbital interaction between its NH_2 group and C4a. This interaction is in agreement with the PN mechanism. On the contrary, this interaction is not observed in both the BA and PEA complexes, indicating that these molecules might not follow the same mechanism. These observations are in agreement with the different charges that should arise for each proposed mechanism, i.e., a more basic N5 for the PN and a more electrophilic N5 for the HT mechanism. Thus, subtle differences in the obtained TS could explain the differential enzyme activities observed for these three substrates with MAO B. According to our results for BA and PEA, it is not possible to

conclude the likelihood of the hydride transfer occurring in one or two steps. Thus, further studies should be done in order to lend additional support to this proposal.

According to our results, it seems that the mechanism by which monoamines are oxidized is strongly dependent on the nature of the substrate. For example, a substituent that can anchor the molecule at the entrance cavity can make this substrate follow a different mechanism. On the other hand, the observed reaction rates (as k_{red} values) can be directly related to the active site amino acids' ability to stabilize the transition state geometries, thus allowing the catalysis to be more efficient with certain substrates. It is also possible to conclude that *p*-substituent effects can profoundly modify a molecule's reactivity not only by altering the reactivity of the ligand toward the flavin moiety but also by establishing additional interactions in the MAO B active site.

■ METHODOLOGY

Computational Details. *The Cluster Approach.* The cluster approach for enzyme catalysis considers a relatively small but well-chosen part of the enzyme (ca. 165 atoms for PEA, 162 atoms for BA, and 164 for NBA) in such a way that the selected cluster behaves and reacts like the real system. Generally, the catalyzed reaction occurs in a small region of the enzyme, and the rest of the enzyme contributes to the catalysis to a lesser extent.

When this methodology is applied two contributions are considered, i.e., the steric constraints imposed by the enzyme on the active site and the long-range polarization effects, which affect the computed energies. To overcome difficulties arising from the first one, all the $C\alpha$'s side chains of residues for MAO B described in the Introduction were locked in their crystallographic positions. Keeping these atoms frozen prevents unrealistic movements of these selected group of atoms. Doing so, this approach guarantees the structural integrity of the model, allowing for some flexibility of these selected groups. As described by Himo,[44] the error introduced by this approximation becomes smaller as the freezing points move further away from the active site.

To overcome long-range polarization effects, solvation effects were considered at the same level of theory as the geometry optimizations carrying out single-point calculations on the optimized structures using the CPC model.[45,46] Two dielectric constants, i.e., $\varepsilon = 4$ and $\varepsilon = 80$, were used in our calculations. The differences in the energy profiles obtained using both dielectric constants are ca. 1.5 kcal mol^{-1} (Table S2, Supporting Information). As stated by Himo,[44] despite the complexity involved in the dielectric constant assignments for active sites, the robustness of the Quantum Chemical Cluster Approach avoids this issue making the cluster selection independent of the dielectric constant, provided that solvation effects converge.[29]

Linear Transit. To reduce the computational time searching for a transition state structure regarding to the quasi-Newton algorithm, it is necessary to select main reaction coordinates such as bond distances, bond angles, or dihedral angles followed by a linear transit scan along the selected coordinate. The highest point obtained in this energy profile as a function of the chosen reaction coordinate is then used for the transition state search. In our case, the LT was chosen between the flavin N5 and the Hα proton of the different substrates.

Cluster Selections. All our models were built using the crystal structure of human MAO B expressed in *Pichia pastoris*

complexed with *p*-nitrobenzylamine (PDB code 2C70).[35] In this crystal structure, NBA is bound to the binding site with its $C\alpha$ side chain pointing toward the isoalloxazine ring. This pose was used to locate the aromatic moieties of the other two deprotonated substrates (BA and PEA) because no crystal structures are available for their interactions with MAO B. The active site models included the isoalloxazine ring of the flavin cofactor and the residues Tyr398 and Tyr435, which form the aromatic cage. Also, Tyr188, Gln206, Lys296, Cys172, Ile199, and Tyr326 were considered according to their known significance in MAO B catalysis. The active site models also incorporated four water molecules present in the crystal structure of MAO B complexed with NBA (these molecules were further verified by using the WaterDock[47] script in the Vina Docking program).

Theoretical Calculations of Free Energies. In the case of the uncatalyzed reaction, the models included the isolated isoalloxazine ring of FAD, isolated substrate (S), complex in its ground state in the solvent cage (FAD-S), and transition state of the complex ([FAD-S]$^{\neq}$). For the catalyzed reaction, the models include the isolated active site, i.e., without substrate (E), the isolated substrate (S), the enzyme substrate complex in its basal state (ES or RC), and finally the transition state of the complex enzyme substrate ([ES]$^{\neq}$ or TS).

All calculations were carried out using the M06-2X functional,[48] highly recommended for thermochemistry and kinetics and because it describes attractive long-range dispersion interactions. This functional is implemented in the Gaussian09 suite of programs.[49] Geometries were optimized using the 6-31G(d,p) basis set. In order to get more accurate energies, single-point calculations were carried out on the optimized geometries using a larger basis set, 6-311+G(2d,2p). Frequencies were computed analytically at the same level of theory as the geometry optimizations to confirm whether the obtained structures were minima or transition states and to obtain zero-point energy (ZPE) corrections. The final energies reported in the present paper are thus the large basis set energies corrected for ZPE, solvation, and dispersion effects. The latter effect is included in the MO6-2X functional. In order to undoubtedly assign reactants and products, we scaled the transition state frequencies, which then were optimized and confirmed as local minima. Imaginary frequencies of the enzymatic transition states were 1134.6*i*, 1089.43*i*, and 1151.23*i* cm^{-1} for BA, NBA, and PEA, respectively. In the case of reactions in solution, frequencies were 915.86*i*, 741.06*i*, and 795.42*i* cm^{-1} for BA, NBA, and PEA, respectively. Covalent adducts were found only for substrates in solution, while the enzymatic product complexes did not show such adducts (see Cartesian Coordinates section, Supporting Information).

Experimental Gibbs Free Energies from Kinetic Rate Constants. Rate constants can be calculated according to the well-known eq 1:

$$k = \frac{k_b T}{hc} e^{-\Delta G^{\neq}/RT} \tag{1}$$

where k = rate constant, k_b = Boltzmann constant, T = temperature, $\Delta G^{\neq}$ = free energy of activation, h = Planck's constant, c = concentration (taken as unity), and R = gas constant. This equation is valid for simple transition state theory where the transmission coefficient is approximated to unity.[32]

Catalytic Power. The catalytic power of the enzyme was evaluated by rearranging the TST equation for catalyzed and

uncatalyzed reactions eq 2. This property is represented in kinetic and energy terms by the ratio k_{cat}/k_{uncat} and $\Delta\Delta G^{\neq}$, respectively.

$$\frac{k_{red}}{k_{uncat}} = e^{\Delta\Delta G^{\neq}/RT} \tag{2}$$

Natural Bond Orbital (NBO) Analysis. The NBO analysis[50−55] provides an accurate Lewis structure picture of a molecule using the highest percentage of orbital electron density representation. As such, this tool allows the understanding of intra- and/or intermolecular interactions mainly gathering information from the interactions occurring between filled and virtual orbitals. Also it derives information regarding charge density changes between atoms, which may act as donors and/or acceptors with regard to a single molecule or to different molecules interacting with each other. This may stabilize the whole system due to the relationship between bonding and antibonding orbitals.[56]

The relationship between donor (*i*) and acceptor (*j*) corresponds to the stabilization energy $E(2)$, which is estimated as eq 3:

$$E(2) = \Delta E_{ij} = q_i \frac{F(i, j)^2}{E_j - E_i} \tag{3}$$

where q_i is the donor orbital occupancy; E_i and E_j are diagonal elements, and $F_{(i,j)}$ is the off diagonal NBO Fock matrix element.

A larger $E(2)$ value corresponds to a stronger interaction between donor and electron acceptor atoms, or in other words, a stronger donating tendency from donor to electron acceptor and consequently a greater extension of the conjugation in the whole system resulting in a stabilization of the system. All calculations were carried out using the NBO 6.0 program.[56]

■ ASSOCIATED CONTENT

Ⓢ Supporting Information

Table S1. Hydrogen Bonds formed at the active site in the reactant complex (RC) and transition state (TS) for BA, NBA, PEA complexed with MAO B. All distances were measured between heavy atoms. The symbol (−) indicates the absence of a hydrogen bond. **Table S2.** The three upper rows display the contributions to free energy of activation for BA, PEA, and NBA complexed with MAO B. The three lower rows display the contributions to free energy of activation in solution (substrate + isoalloxazine ring). **Figure S1.** Intramolecular natural bond orbitals taken from second-order perturbation theory involved in the reactivity and stabilization of NBA–flavin interaction. (a) C4a orbital interacting with the C10a–N1 bond orbital. (b) C4a orbital interacting with the N5 and the transferred proton. (c) N5's lone pair orbital interacting with the C4a–C10a bond orbital. (d) N10 orbital interacting with C10a–N1 bond orbital through its lone pair donation. **Figure S2.** Water–flavin NBO orbitals taken from second-order perturbation theory involved in the stabilization and reactivity of the system. **Figure S2.** (a) and (b) display the interaction between the water molecule lone pairs toward the oxygen atom pointing to C4 and a hydrogen atom of the −NH₂ substrate moiety. (c) Depicted is the stabilizing interaction between N1 and a water molecule. (d) The N1–C10a bond is also stabilized by a water molecule. **Figure S3.** Water–NBA NBO orbitals taken from second-order perturbation theory involved in the stabilization and reactivity of the system. The

figure depicted the interaction described between water oxygen lone pair stabilizing an antibonding orbital of the N−H bond of the substrates amine moiety. **Figure S4.** Intramolecular NBO orbitals taken from second-order perturbation theory involved in the reactivity and stabilization of PEA−MAO B complex. **Figure S4.** (a) and (b) display how N5's lone pair stabilizes antibonding orbitals of bonds formed by N5−C4a and C4a−C10a. (c) Displayed is how the N1−C10a bond donates electronic density toward the antibonding orbital of C4a−N5 bond. (d) Stabilizing interaction of C4a−N5 bond between its bonding and antibonding orbitals. (e) N10s lone pair stabilizing the antibonding orbital of N1−C10a bond. The Supporting Information is available free of charge on the ACS Publications website at DOI: 10.1021/acs.jcim.5b00140.

■ AUTHOR INFORMATION

Corresponding Author

*Phone: + 56 2-2 9782843. E-mail: gzapata@uchile.cl. (Gerald Zapata-Torres)

Notes

The authors declare no competing financial interest.

■ REFERENCES

(1) Gaweska, H.; Fitzpatrick, P. H. Structures and Mechanism of the Monoamine Oxidase Family. *BioMol. Concepts* **2011**, *2*, 365−377.

(2) Edmondson, D. E.; Binda, C.; Wang, J.; Upadhyay, A. K.; Mattevi, A. Molecular and Mechanistic Properties of Membrane-Bound Mitochondrial Monoamine Oxidases. *Biochemistry* **2009**, *48*, 4220−4230.

(3) Miller, J. R.; Edmondson, D. E. Structure-Activity Relationships in the Oxidation of Para-Substituted Benzylamine Analogues by Recombinant Human Liver Monoamine Oxidase A. *Biochemistry* **1999**, *38*, 13670−13683.

(4) Silverman, R. B. Radical Ideas about Monoamine Oxidase. *Acc. Chem. Res.* **1995**, *28*, 335−342.

(5) Lu, X.; Ji. H.; Silverman, R. B. *In Flavins and Flavoproteins*; Chapman, S., Perham, R., Scrutton, N., Eds.; Rudolf Weber Agency for Scientific Publications: Berlin, 2002; pp 817−830.

(6) Fitzpatrick, P. F. Oxidation of Amines by Flavoproteins. *Arch. Biochem. Biophys.* **2010**, *493*, 13−25.

(7) Vianello, R.; Repič, M.; Mavri, J. How are Biogenic Amines Metabolized by Monoamine Oxidases? *Eur. J. Org. Chem.* **2012**, *36*, 7057−7065.

(8) Orru, R.; Adelco, M.; Edmondson, D. E. Do MAO A and MAO B Utilize the Same Mechanism for the C-H Bond Cleavage Step in Catalysis? Evidence Suggesting Differing Mechanism. *J. Neural Transm.* **2013**, *120*, 847−851.

(9) Malcomson, T.; Yelekci, K.; Borrello, M. T.; Ganesan, A.; De Kimpe, N.; Semina, E.; Mangelinckx, S.; Ramsay, R. R. cis-Cyclopropylamines as Mechanism-Based Inhibitors of Monoamine Oxidases. *FEBS J.* **2015**, DOI: 10.1111/febs.13260.

(10) Erdem, S. S.; Büyükmenekse, B. Computational Investigation on the Structure-Activity Relationship of the Biradical Mechanism for Monoamine Oxidase. *J. Neural Transm.* **2011**, *118*, 1021−1029.

(11) Abad, E.; Zenn, R. K.; Kästner, J. Reaction Mechanism of Monoamine Oxidase from QM/MM Calculations. *J. Phys. Chem. B* **2013**, *117*, 14238−14246.

(12) Akyüz, M. A.; Erdem, S. S. Computational Modeling of the Direct Hydride Transfer Mechanism for the MAO Catalyzed Oxidation of Phenethylamine and Benzylamine: ONIOM (QM/QM) Calculations. *J. Neural Transm.* **2013**, *120*, 937−945.

(13) Repič, M.; Vianello, R.; Purg, M.; Duarte, F.; Bauer, P.; Kamerlin, S. C. L.; Mavri, J. Empirical Valence Bond Simulations of the Hydride Transfer Step in the Monoamine Oxidase B Catalyzed Metabolism of Dopamine. *Proteins: Struct., Funct., Bioinf.* **2014**, *82*, 3347−3355.

(14) Akyüz, M. A.; Erdem, S. S.; Edmondson, E. D. The Aromatic Cage in the Active Site of Monoamine Oxidase B: Effect on the Structural and Electronic Properties of Bound Benzylamine and *p*-Nitrobenzylamine. *J. Neural Transm.* **2007**, *114*, 693−698.

(15) Pless, S. A.; Hanek, A. P.; Price, K. L.; Lynch, J. W.; Lester, H. A.; Dougherty, D. A.; Lummis, S. C. R. A Cation-*π* Interaction at a Phenylalanine Residue in the Glycine Receptor Binding Site is Conserved for Different Agonists. *Mol. Pharmacol.* **2011**, *79*, 742−748.

(16) Zapata-Torres, G.; Fierro, A.; Miranda-Rojas, S.; Guajardo, C.; Saez-Briones, P.; Salgado, J. C.; Celis-Barros, C. Influence of Protonation on Substrate and Inhibitor Interactions at the Active Site of Human Monoamine Oxidase-A. *J. Chem. Inf. Model.* **2012**, *52*, 1213−1221.

(17) Repič, M.; Purg, M.; Vianello, R.; Mavri, J. Examining Electrostatic Preorganization in Monoamine Oxidases A and B by Structural Comparison and pK_a Calculations. *J. Phys. Chem. B* **2014**, *118*, 4326−4332.

(18) Binda, C.; Mattevi, A.; Edmondson, D. E. Structure-Function Relationships in Flavoenzyme-Dependent Amine Oxidations: A Comparison of Polyamine Oxidase and Monoamine Oxidase. *J. Biol. Chem.* **2002**, *277*, 23973−23976.

(19) Karasulu, B.; Patil, M.; Thiel, W. Amine Oxidation Mediated by Lysine-Specific Demethylase 1: Quantum Mechanics/Molecular Mechanics Insights into Mechanism and Role of Lysine 661. *J. Am. Chem. Soc.* **2013**, *135*, 13400−13413.

(20) Kong, X.; Ouyang, S.; Liang, Z.; Lu, J.; Cheng, L.; Sheng, B.; Li, D.; Zheng, M.; Li, K. K.; Luo, C.; Jiang, H. Catalytic Mechanism Investigation of Lysine-Specific Demethylase 1 (LSD1): A Computational Study. *PLoS One* **2001**, *6*, e25444.

(21) Borštnar, R.; Repič, M.; Kamerlin, S. C. L; Vianello, R.; Mavri, J. Computational Study of the pK_a Values of Potential Catalytic Residues in the Active Site of Monoamine Oxidase B. *J. Chem. Theory Comput.* **2012**, *10*, 3864−3870.

(22) Wang, J.; Edmondson, D. E. [2]H Kinetic Isotope Effects and pH Dependence of Catalysis as Mechanistic Probes of Rat Monoamine Oxidase A: Comparisons with the Human Enzyme. *Biochemistry* **2011**, *50*, 7710−7717.

(23) MacMillar, S.; Edmondson, D. E.; Matsson, O. Nitrogen Kinetic Isotope Effects for the Monoamine Oxidase B-Catalyzed Oxidation of Benzylamine and (1, 1-[2]H$_2$) Benzylamine: Nitrogen Rehybridization and CH Bond Cleavage are Not Concerted. *J. Am. Chem. Soc.* **2011**, *133*, 12319−12321.

(24) Zenn, K. R.; Abad, E.; Kästner, J. Influence of the Environment on the Oxidative Deamination of *p*-Subtituted Benzylamines in Monoamine Oxidase. *J. Phys. Chem. B* **2015**, *119*, 3678−3686.

(25) Erdem, S. S.; Karahan, Ö.; Yıldız, I.; Yelekçi, K. A Computational Study on the Amine-Oxidation Mechanism of Monoamine Oxidase: Insight into the Polar Nucleophilic Mechanism. *Org. Biomol. Chem.* **2006**, *4*, 646−658.

(26) Atalay, V. E.; Erdem, S. S. A Comparative Computational Investigation on the Proton and Hydride Transfer Mechanisms of Monoamine Oxidase Using Model Molecules. *Comput. Biol. Chem.* **2013**, *47*, 181−191.

(27) Edmondson, D. E.; Bhattacharyya, A. K.; Walker, M. C. Spectral and Kinetic Studies of Imine Product Formation in the Oxidation of p-(N,N-dimethylamino)benzylamine Analogs by Monoamine Oxidase B. *Biochemistry* **1993**, *19*, 5196−5202.

(28) Edmondson, D. E. Structure Activity Studies of the Substrate Binding Site in Monoamine Oxidase B. *Biochimie* **1995**, *7−8*, 643−650.

(29) Siegbahn, P. E.; Himo, F. Recent Developments of the Quantum Chemical Cluster Approach for Modeling Enzyme Reactions. *J. Biol. Inor. Chem.* **2009**, *14*, 643−651.

(30) Lind, M. E. S.; Himo, F. Theoretical Study of Reaction Mechanism and Stereoselectivity of Arylmalonate Decarboxylase. *ACS Catal.* **2014**, *4*, 4153−4160.

(31) Siegbahn, P. E. M.; Himo, F. Review: The Quantum Chemical Cluster Approach for Modeling Enzyme Reactions. *WIREs Comput. Mol. Sci.* **2011**, *1*, 323−336.

(32) Anslyn, E. V.; Dougherty, D. A., Eds.; *Modern Physical Organic Chemistry*; University Science Books: Herndon, VA, 2006.

(33) Miller, J. R.; Edmondson, D. E. Structure Activity Relationships in the Oxidation of Para-Substituted Benzylamine Analogues by Recombinant Human Liver Monoamine Oxidase A. *Biochemistry* **1999**, *38*, 13670−13683.

(34) Husain, M.; Edmondson, D. E.; Singer, T. P. Kinetic Studies on the Catalytic Mechanism of Liver Monoamine Oxidase. *Biochemistry* **1982**, *21*, 595−600.

(35) Li, M.; Binda, C.; Mattevi, A.; Edmonson, D. E. Functional Role of the "Aromatic Cage" in Human Monoamine Oxidase B: Structures and Catalytic Properties of Tyr435 Mutant Proteins. *Biochemistry* **2006**, *45*, 4775−4784.

(36) Liao, R. Quantum Chemical Cluster Modeling of Enzymatic Reactions; Ph.D. Thesis, Stockholm University, Stockholm, Sweden, 2010. http://www.diva-portal.org/smash/get/diva2:353152/FULLTEXT01.pdf (accessed June 2015).

(37) Giraldo, J.; Roche, D.; Rovira, X.; Serra, J. The Catalytic Power of Enzymes: Conformational Selection or Transition State Stabilization? *FEBS Lett.* **2006**, *580*, 2170−2177.

(38) Warshel, A.; Sharma, P. K.; Kato, M.; Xiang, Y.; Liu, H.; Olsson, M. H. Electrostatic Basis for Enzyme Catalysis. *Chem. Rev.* **2006**, *106*, 3210−3235.

(39) McGaughey, G. B.; Gagné, M.; Rappé, A. K. *π*-Stacking Interactions Alive and Well in Proteins. *J. Biol. Chem.* **1998**, *273*, 15458−15463.

(40) Milczek, E. M.; Binda, C.; Rovida, S.; Mattevi, A.; Edmondson, D. E. The 'Gating' Residues Ile199 and Tyr326 in Human Monoamine Oxidase B. Function in Substrate and Inhibitor Recognition. *FEBS J.* **2011**, *278*, 4860−4869.

(41) Pozzi, M. H.; Fitzpatrick, P. F. A Lysine Conserved in the Monoamine Oxidase Family is Involved in Oxidation of the Reduced Flavin in Mouse Polyamine Oxidase. *Arch. Biochem. Biophys.* **2010**, *498*, 83−88.

(42) Geha, R. M.; Chen, K.; Wouters, J.; Ooms, F.; Shih, J. C. Analysis of Conserved Active Site Residues in Monoamine Oxidase A and B and their Three-Dimensional Molecular Modeling. *J. Biol. Chem.* **2002**, *277*, 17209−17216.

(43) Bodnarchuk, M. S.; Viner, R.; Michel, J.; Essex, J. W. Strategies to Calculate Water Binding Free Energies in Protein−Ligand Complexes. *J. Chem. Inf. Model.* **2014**, *54*, 1623−1633.

(44) Himo, F. Quantum Chemical Modeling of Enzyme Active Sites and Reaction Mechanisms. *Theor. Chem. Acc.* **2006**, *116*, 232−240.

(45) Cossi, M.; Rega, N.; Scalmani, G.; Barone, V. Energies, Structures, and Electronic Properties of Molecules in Solution with the C-PCM Solvation Model. *J. Comput. Chem.* **2003**, *24*, 669−681.

(46) Barone, V.; Cossi, M. Quantum Calculation of Molecular Energies and Energy Gradients in Solution by a Conductor Solvent Model. *J. Phys. Chem. A* **1998**, *102*, 1995−2001.

(47) Ross, G. A.; Morris, G. M.; Biggin, P. C. Rapid and Accurate Prediction and Scoring of Water Molecules in Protein Binding Sites. *PLoS One* **2012**, *7*, e32036.

(48) Zhao, Y.; Truhlar, D. G. The M06 Suite of Density Functionals for Main Group Thermochemistry, Thermochemical Kinetics, Noncovalent Interactions, Excited States, and Transition Elements: Two New Functionals and Systematic Testing of Four M06-Class Functionals and 12 Other Functionals. *Theor. Chem. Acc.* **2008**, *120*, 215−241.

(49) Frisch, M. J.; Trucks, G. W.; Schlegel, H. B.; Scuseria, G. E.; Robb, M. A.; Cheeseman, J. R.; Scalmani, G.; Barone, V.; Mennucci, B.; Petersson, G. A.; Nakatsuji, H.; Caricato, M.; Li, X.; Hratchian, H. P.; Izmaylov, A. F.; Bloino, J.; Zheng, G.; Sonnenberg, J. L.; Hada, M.; Ehara, M.; Toyota, K.; Fukuda, R.; Hasegawa, J.; Ishida, M.; Nakajima,

T.; Honda, Y.; Kitao, O.; Nakai, H.; Vreven, T.; Montgomery, J. A., Jr.; Peralta, J. E.; Ogliaro, F.; Bearpark, M.; Heyd, J. J.; Brothers, E.; Kudin, K. N.; Staroverov, V. N.; Kobayashi, R.; Normand, J.; Raghavachari, K.; Rendell, A.; Burant, J. C.; Iyengar, S. S.; Tomasi, J.; Cossi, M.; Rega, N.; Millam, J. M.; Klene, M.; Knox, J. E.; Cross, J. B.; Bakken, V.; Adamo, C.; Jaramillo, J.; Gomperts, R.; Stratmann, R. E.; Yazyev, O.; Austin, A. J.; Cammi, R.; Pomelli, C.; Ochterski, J. W.; Martin, R. L.; Morokuma, K.; Zakrzewski, V. G.; Voth, G. A.; Salvador, P.; Dannenberg, J. J.; Dapprich, S.; Daniels, A. D.; Farkas, Ö.; Foresman, J. B.; Ortiz, J. V.; Cioslowski, J.; Fox, D. J. *Gaussian 09*, Revision D.01; Gaussian, Inc.: Wallingford, CT, 2009.

(50) Foster, J. P.; Weinhold, F. Natural Hybrid Orbitals. *J. Am. Chem. Soc.* **1980**, *102*, 7211−7218.

(51) Reed, A. E.; Weinhold, F. Natural Bond Orbital Analysis of Near-Hartree−Fock Water Dimer. *J. Chem. Phys.* **1983**, *78*, 4066− 4073.

(52) Reed, A. E.; Weinstock, R. B.; Weinhold, F. Natural population analysis. *J. Chem. Phys.* **1985**, *83*, 735−746.

(53) Reed, A. E.; Weinhold, F. Natural Localized Molecular Orbitals. *J. Chem. Phys.* **1985**, *83*, 1736−1740.

(54) Reed, A. E.; Curtiss, L. A.; Weinhold, F. Intermolecular Interactions from A Natural Bond Orbital, Donor-Acceptor Viewpoint. *Chem. Rev.* **1988**, *88*, 899−926.

(55) Li, L.; Wu, C.; Wang, Z.; Zhao, L.; Li, Z.; Sun, C.; Sun, T. Density Functional Theory (DFT) and Natural Bond Orbital (NBO) Study of Vibrational Spectra and Intramolecular Hydrogen Bond Interaction of L-Ornithine−L-Aspartate. *Spectrochim. Acta, Part A* **2015**, *136*, 338−346.

(56) Glendening, E. D.; Badenhoop, J. K.; Reed, A. E.; Carpenter, J. E.; Bohmann, J. A.; Morales, C. M.; Landis, C. R.; Weinhold, F. NBO 6.0; Theoretical Chemistry Institute: University of Wisconsin, Madison, WI, 2013.